TOXICOLOGICAL SCIENCES **124(2)**, 487–501 (2011)
doi:10.1093/toxsci/kfr238
Advance Access publication September 13, 2011

Toxicogenomics and Metabolomics of Pentamethylchromanol (PMCol)-Induced Hepatotoxicity

Toufan Parman,*[,1] Deborah I. Bunin,* Hanna H. Ng,* Jonathan E. McDunn,† Jacob E. Wulff,† Abraham Wang,* Robert Swezey,* Laura Rasay,* David G. Fairchild,* Izet M. Kapetanovic,‡ and Carol E. Green*

*Biosciences Division, SRI International, Menlo Park, California 94025-3493; †Research and Development, Metabolon, Inc., Durham, North Carolina 27113; and ‡Chemopreventive Agent Development Research Group, Division of Cancer Prevention, National Cancer Institute, Bethesda, Maryland 20892

[1]To whom correspondence should be addressed at Biosciences Division, SRI International, 333 Ravenswood Avenue, Menlo Park, CA 94025-3493. Fax: (650) 859-3444. E-mail: toufan.parman@sri.com.

Received June 1, 2011; accepted September 5, 2011

Pentamethyl-6-chromanol (PMCol), a chromanol-type compound related to vitamin E, was proposed as an anticancer agent with activity against androgen-dependent cancers. In repeat dose-toxicity studies in rats and dogs, PMCol caused hepatotoxicity, nephrotoxicity, and hematological effects. The objectives of this study were to determine the mechanisms of the observed toxicity and identify sensitive early markers of target organ injury by integrating classical toxicology, toxicogenomics, and metabolomic approaches. PMCol was administered orally to male Sprague-Dawley rats at 200 and 2000 mg/kg daily for 7 or 28 days. Changes in clinical chemistry included elevated alanine aminotransferase, total bilirubin, cholesterol and triglycerides—indicative of liver toxicity that was confirmed by microscopic findings (periportal hepatocellular hydropic degeneration and cytomegaly) in treated rats. Metabolomic evaluations of liver revealed time- and dose-dependent changes, including depletion of total glutathione and glutathione conjugates, decreased methionine, and increased S-adenosylhomocysteine, cysteine, and cystine. PMCol treatment also decreased cofactor levels, namely, FAD and increased NAD(P)+. Microarray analysis of liver found that differentially expressed genes were enriched in the glutathione and cytochrome P450 pathways by PMCol treatment. Reverse transcription-polymerase chain reaction of six upregulated genes and one down-regulated gene confirmed the microarray results. In conclusion, the use of metabolomics and toxicogenomics demonstrates that chronic exposure to high doses of PMCol induces liver damage and dysfunction, probably due to both direct inhibition of glutathione synthesis and modification of drug metabolism pathways. Depletion of glutathione due to PMCol exposure ultimately results in a maladaptive response, increasing the consumption of hepatic dietary antioxidants and resulting in elevated reactive oxygen species levels associated with hepatocellular damage and deficits in liver function.

Key Words: **pentamethylchromanol; gene expression; metabolomics; hepatotoxicity; glutathione; toxicogenomic.**

Vitamin E has been widely investigated as a chemopreventative agent for its antioxidant properties and has shown activity against bladder (Liang *et al.*, 2008) and mammary cancer (Sharhar *et al.*, 2008; Shen *et al.*, 2008; Suh *et al.*, 2007). Chromanol-type compounds, including vitamin E, act as antioxidants in biological systems by reduction of oxygen-centered radicals (Gregor *et al.*, 2005; Tyurina *et al.*, 1995). Based on these antioxidant properties, α-tocopherol and its analogs are candidate therapies for the prevention and treatment of various chronic illnesses, including cancer and cardiovascular disease. For example, 2,2,5,7,8-pentamethyl-6-chromanol (PMCol, Fig. 1) has been shown to have antiandrogenic activity in prostate carcinoma cells (Thompson and Wilding, 2003) and may be efficacious against other cancers as well (Liang *et al.*, 2008; Shen *et al.*, 2008). PMCol consists of the Chromanol ring of vitamin E without the lipophilic phytyl tail and therefore is proposed as a more effective and practical analog of vitamin E because of its increased water solubility while still retaining the antioxidant characteristics of vitamin E (Thompson and Wilding, 2003).

The toxicity of PMCol has been studied in both rats and dogs after 28 days of oral dose administration as part of a preclinical development program to advance PMCol as a cancer chemopreventive agent (Lindeblad *et al.*, 2010a, 2010b). These studies demonstrated that daily administration of the drug candidate resulted in pronounced toxicity in both species. In rats given doses of 500 and 2000 mg/kg/day, hepatotoxicity, nephrotoxicity, and anemia were observed. In dogs, the primary target organs were liver and thymus. Like vitamin E (Abdo *et al.*, 1986), PMCol was toxic to several organs at high doses, but the mechanism of these adverse effects is largely unknown.

The application of nontargeted approaches of genomics, proteomics, and metabolomics to toxicity assessments is proving valuable, especially for classic problems related to target organ toxicity. For example, metabolomics, applying liquid-chromatography–tandem mass spectrometry (LC/MS/MS) and gas chromatography–mass spectrometry (GC/MS) platforms to monitor metabolic small-molecule changes across a wide range of biochemical pathways, has identified markers of nephrotoxicity (Boudonck *et al.*, 2009) and highlighted

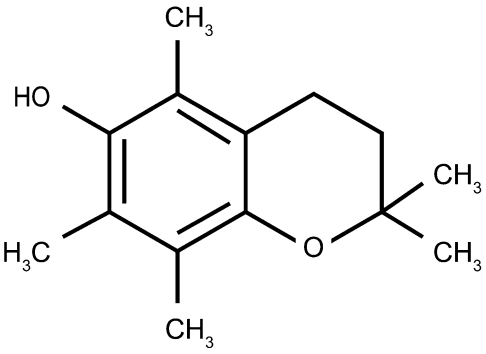

FIG. 1. The chemical structure of PMCol

a potential mechanism of action for ethylene glycol monomethyl ether toxicity (Takei *et al.*, 2010). Toxicogenomics using microarray technology to monitor biological samples for transcriptional changes has also proven valuable for characterizing toxicity; for example, Gao *et al.* (2010) used these techniques to define mechanism-related biomarker gene sets for hepatotoxicity. These approaches, combined with classic toxicity assessment endpoints, can provide insight into the mechanisms of drug action and/or toxicity as well as identify biomarkers useful for toxicity monitoring—all of which are critical for the drug development process and may be important in clinical practice.

In the current study, male rats received vehicle control or PMCol at doses of 200 (low dose) or 2000 mg/kg/day (high dose) orally for 7 or 28 consecutive days. Signs of PMCol-induced toxicity were monitored using traditional toxicity assessments (e.g., clinical pathology and histopathology), and these results were integrated with a metabolomics investigation of liver, kidney, and plasma. In addition, microarray toxicogenomic analysis was used to determine differentially expressed genes in liver after PMCol administration. Together, these data demonstrate that PMCol-induced hepatotoxicity most likely results from severe glutathione depletion. Metabolomic and toxicogenomic evaluations also identified changes in several metabolic products (e.g., methionine, cysteine, and glutathione) and genes (e.g., Akr7a3 and Gstp1) in the glutathione metabolism pathway as potential early markers of PMCol-induced liver toxicity.

MATERIALS AND METHODS

Test System

A total of 30 male (6/group) Crl:CD Sprague-Dawley Virus Antibody Free rats (Harlan, Livermore, CA) at 6–7 weeks of age were maintained on Purina Certified Rodent Chow 5002 (Richmond, IN) and reverse osmosis purified tap water *ad libitum* under controlled lighting (12-h light-dark cycle). Animals were housed (3 per cage) in microisolator cages in an Association for Assessment and Accreditation of Laboratory Animal Care, International (AAALAC) accredited animal facility, and their use was approved by the facility Institutional Animal Care and Use Committee (IACUC).

Study Design

The 28-day oral dose study in male rats was performed to assess general toxicity, toxicogenomic, and metabolomics of PMCol. After a three-day quarantine period, body weights were measured at randomization, and animals were assigned to dose groups. Rats were administered vehicle or PMCol by once daily oral gavage at a volume of 10 ml/kg/day and at concentrations of 0, 200, and 2000 mg/kg/day. Selection of these doses was based on the results of the previous toxicity study in rats (Lindeblad *et al.*, 2010a), which indicated that the two doses, 200 and 2000 mg/kg, would cause adverse effects in the target tissues in a dose-dependent manner, optimizing the likelihood of identification of an early marker for hepatotoxicity and nephrotoxicity. The vehicle and high-dose groups were euthanized on day 8 ($n = 6$ rats/group). Separate cohorts of 6 rats/group in the vehicle, low-, and high-dose groups were euthanized on day 29.

Body weights were recorded on day 1, once weekly thereafter, and at each necropsy. Rats were examined twice daily for clinical signs of toxicity (within approximately 30 min of dose administration and approximately 4–5 h postdose) and once a week for detailed clinical signs and symptoms. Food consumption was quantitatively measured for an approximately 24 h period at pretest and once weekly. Plasma for drug level determination was collected from nonfasted animals ~2 h after the last dose on days 7 and 28. After collection of plasma for drug levels, animals were fasted for at least 3–4 h before they entered metabolism cages for urine collection. On days 8 and 29, blood, plasma, and urine samples were collected from fasted rats before euthanization and evaluated for clinical pathology, metabolomics, and total protein analysis. Urine was collected overnight in metabolism cages at ambient temperature, without the use of any antibacterial agent. After gross necropsy, kidney and liver weights were determined, and samples from each tissue were collected for metabolomics and histopathology. Only liver samples were used for toxicogenomics assessment.

Test Article

Pentamethylchromanol (2,2,5,7,8-Pentamethyl-6-chromanol, PMCol), an off-white solid, was supplied by Division of Cancer Prevention Repository c/o Fisher BioServices (Germantown, MD) and refrigerated. The purity was determined by high performance liquid chromatography (HPLC) before initiation of dosing and after completion of the in-life phase to confirm test article stability over the course of the study.

Preparation and analysis of test substance. The test article formulations were prepared in 1% aqueous methyl cellulose (vehicle, Sigma-Aldrich, Saint Louis, MO) and were tested for concentration and homogeneity using the following HPLC method: Discovery C18, 150 × 4.6 mm, 5 µm column (Supelco, Bellefonte, PA) with a 2.0-ml/min flow rate, 10-µl injection volume, detection at 295 nm, and water:acetonitrile mobile phases ([A] 95:5 and [B] 10:90 vol/vol). Elutions were isocratic (80:20%) for the first and last 4 min of the run and gradient (25:75%) at 7.7 and 15 min. Dose formulations were considered to be stable under refrigeration for at least 6 days (Lindeblad *et al.*, 2010a).

Clinical Pathology

Standard methods were used to measure hematology and clinical chemistry parameters and total urine protein (Advia 120 Analyzer, Bayer HealthCare, Tarrytown, NY and Cobas c501 Chemistry Analyzer, Roche Diagnostics, Indianapolis, IN).

Plasma Drug Levels

Plasma samples were processed by protein precipitation with acetonitrile and the supernatants were analyzed by LC-MS/MS. Samples were injected onto a Luna C18(2) column (50 × 2.00 mm; 3 µm; Phenomenex, Torrance, CA) with a mobile phase A (0.1% formic acid in water) and mobile phase B (0.1% formic acid in acetonitrile) and eluted at a flow rate of 0.3 ml/min with the following gradient conditions: 0 and 8 min 50% A and 50% B; 8.5 and 20 min 10% A and 90% B; and 20.1 and 24 min 50% A and 50% B. Quantification was performed using a Micromass Quattro LC Mass Spectrometer (Waters, Milford,

MA) operating in positive ion mode monitoring the multiple-reaction ion transition of m/z 221.1 to m/z 165.1. The desolvation temperature was 400°C, the capillary voltage was 1.5 kV, the cone voltage was 20 V, and the collision energy was 17 eV.

Metabolomic Profiling

Plasma, urine, 100 mg of the right kidney (no specific region was selected), and 100 mg of the liver left lobe were collected from fasted rats on days 8 and 29, snap frozen, and stored at ≤ -60°C until metabolomic analysis. After cold methanol extraction and mechanical disaggregation, the samples were split into three aliquots for untargeted metabolic profiling. Samples were processed and characterized using three independent platforms: ultrahigh-performance liquid-chromatography/tandem mass spectrometry (UHPLC/MS/MS) in the negative ion mode optimized for basic species, UHPLC/MS/MS in the positive ion mode optimized for acidic species, and GC/MS after sialylation. The details of these platforms were as previously described (Evans *et al*., 2009; Sha *et al*., 2010). The reproducibility of the extraction protocol was assessed by the recovery of xenobiotic compounds spiked into every tissue sample prior to extraction. Chromatographic timelines were standardized based on the elution intervals of these xenobiotics. The technical variability of each analytical platform was assessed by repeated characterization of a pooled standard that contained an aliquot of each sample within the study.

Toxicogenomic Sample Preparation and Data Analysis

The remaining portion of the liver left lobe was cut into ≤ 0.3 cm cubed sections and stored submerged in RNAlater (Applied Biosystems, Carlsbad, CA). Liver samples (approximately 20–50 mg) were homogenized using Qiagen's TissueLyser and 5-mm stainless steel beads (Valencia, CA). Total RNA was extracted and purified using the RiboPure and TURBO DNA-*free* kits (Applied Biosystems) with 1-bromo-3-chloropropane (Sigma-Aldrich). RNA quality and integrity was assessed using the RNA 6000 Nano LabChip kit and 2100 Bioanalyzer with 2100 Expert Software (Agilent Technologies, Santa Clara, CA). Total RNA (150 ng) from samples with an RNA integrity number of ≥ 7.0 was processed using the Ambion Whole Transcript (WT) Expression kit (Applied Biosystems) and GeneChip WT Terminal Labeling kit (Affymetrix, Santa Clara, CA). Concentrations were determined with an ND-1000 spectrophotometer (Thermo Scientific, Wilmington, DE). Hybridization and scanning to GeneChip Rat Gene 1.0 ST Arrays were performed as described in the Affymetrix GeneChip WT Sense Target Labeling Assay, revision 5 (http://www.affymetrix.com/support/technical/manuals.affx).

The Affymetrix Rat Gene 1.0 ST CEL files were analyzed using GeneSpring GX11.0 software (Agilent Technologies). Data samples were subjected to quality control by calculating principal component analysis scores and visually representing those scores in a three-dimensional scatter plot (Supplementary fig. 1). Per-gene normalization was applied to normalize the expression level around the value of 1 (base 2 log transformed to 0). GeneChip probe sets were filtered on the basis of their signal intensity values such that at least 6 of the 29 samples had intensity values within the 20 percentile low cutoff range and the 100 percentile high cutoff range. The resulting 22,416 qualified probes (from a total of 27,342 on the GeneChip) were selected for subsequent analysis including fold changes of gene expression and gene set enrichment analysis (GSEA). The data discussed in this publication have been deposited at the National Center for Biotechnology Information Gene Expression Omnibus (GEO Series access number GSE29673, http://www.ncbi.nlm.nih.gov/geo/).

Validation of Gene Expression Data by Real-time PCR

Oligonucleotide primer pairs (Integrated DNA Technologies, San Diego, CA) were designed using ProbeFinder version 2.45 (Roche Diagnostics) to span an intron for each of the eight target rat transcripts (Supplementary table 1). Primers and probes were used at a final concentration of 400nM and 200nM, respectively, in duplicate 20-µl PCR reaction wells with oligo(dT) primed single-stranded complementary DNA (cDNA) template representing a 15 ng total RNA equivalent (SuperScript III First-Strand Synthesis SuperMix kit, Invitrogen, Carlsbad, CA). The LightCycler 480 96-well instrument and associated software (version 1.5.0 SP3), LightCycler 480 Probes Master reagent, Universal ProbeLibrary FAM-labeled hydrolysis probes, and glyceraldehyde-3-phosphate dehydrogenase (Gapdh) hydrolysis probes and primers were all from Roche Applied Sciences and Diagnostics. The thermal cycling conditions were denaturation for 10 min at 95°C, followed by 50 cycles of 95°C for 10 s, 60°C for 30 s, and 72°C for 1 s with data acquisition at the end of each 60°C incubation step. Reactions without reverse transcriptase were included to confirm the absence of amplifiable genomic DNA. Gene expression fold changes were calculated using the relative expression ratio method using REST 2009 software (Pfaffl, 2001; Pfaffl *et al*., 2002). A standard curve for each primer pair was created from serially diluted cDNA for use in determining the amplification efficiency of each transcript.

Histopathology

The liver (not including the left lobe) and the remainder of the right kidney were collected, formalin-fixed, embedded in paraffin, cut approximately 5 µm thick, and stained with hematoxylin and eosin for histopathologic examination by a board-certified veterinary pathologist.

Statistical Analysis and Software

Mean and SD were calculated for body weight, food consumption, clinical pathology, and organ weight data at each evaluation interval (Labcat In-Life version 8.2, Labcat Clinical Pathology version 4.42, Labcat Histopathology version 4.32, Labcat Organ Weight version 3.24, Microsoft Excel, 2003 or 2007). Body weights, organ weights, and clinical pathology data were evaluated by one-way ANOVA, followed by Dunnett's *t*-test (if the ANOVA was significant). All other numerical parameters were evaluated by Student's *t*-test, unless specified otherwise.

Statistical analysis of the metabolomic data was performed using the freely available program "R" (http://cran.rproject.org/). Missing values, if any, for a given metabolite were assumed to be below the level of detection and were imputed with the lowest observed abundance for that metabolite from the entire data set. Welch's two-sample *t*-test comparisons between experimental groups were performed on natural log-transformed data ($p \leq 0.05$). Metabolomic data were normalized. The data produced is known as relative quantitation. This is to say that while the measured value of a compound from a single sample does not give any information about the exact amount actually present, the relative values from one sample to another are measurable. For example, if a compound was measured at 10,000 in one sample and 20,000 in the second sample, one can be extremely confident that the true amount of the second sample is twice that of the first. Due to the size of the study, the samples were run over multiple days with the study design being balanced across each of the run days. Following data collection, a "block correction" was performed whereby the values from each run day were rescaled to have median equal to 1. Missing values were then imputed with the minimum.

T-test and Benjamini-Hochberg Multiple Testing Correction were used in the statistical analysis of microarray gene sets (p value ≤ 0.05).

RESULTS

Toxicity Assessment

Clinical signs. PMCol at doses of 200 or 2000 mg/kg/day for 28 days did not result in mortality. Clinical signs were minor and consisted of shoveling, urine stains, and soft stool. PMCol had no adverse effect on body weight and food consumption.

Clinical pathology. Treatment with PMCol resulted in clinical chemistry changes mainly in the 2000 mg/kg/day group on day 8 and/or day 29 (Table 1A). These changes included increases in alanine aminotransferase, triglycerides, total bilirubin, cholesterol, calcium, and globulin as well as a decrease in glucose; all of these changes suggest an adverse effect on the

liver (Table 1A). Alterations in the hematology parameters were subtle and included slight decreases in hematocrit, red blood cell count, hemoglobin, and percent neutrophils, as well as increases in percent and total monocytes, total neutrophils, white blood cell count, platelet count, and percent reticulocytes (Table 1B). All other hematology and clinical chemistry parameters were within the control group ranges.

Organ weights. Absolute liver weight (11.7 ± 0.86 g) and liver weight corrected for body weight (5.75 ± 0.37%) were significantly increased for rats in the 2000 mg/kg/day treatment group on day 8 compared with the control values of 8.24 ± 0.58 g and 3.69 ± 0.22%, respectively. On day 29, significant dose-dependent increases in liver absolute weight and liver weight corrected for body weight were observed for rats treated with 200 mg/kg/day (12.00 ± 0.98 g; 4.09 ± 0.25%) and 2000 mg/kg/day (17.08 ± 1.71 g, 5.76 ± 0.49%) PMCol, compared with the control group (9.38 ± 0.88 g; 2.98 ± 0.19%).

On day 8, a subtle but statistically significant decrease in the kidney weight was noted in the 2000 mg/kg/day treatment group; however, this change was not supported by similar changes in the kidney corrected for body weight value, and it was not present in animals euthanized on day 29.

Pathology. On day 8, mild to moderate periportal hepatocellular hydropic degeneration (in five of six livers) and minimal to mild cytomegaly (in six of six livers) were associated with administration of PMCol at 2000 mg/kg/day. On day 29, minimal to mild cytomegaly was present in rats given PMCol at 200 and 2000 mg/kg/day (in four of six and five of five livers, respectively), whereas minimal to mild periportal hepatocellular hydropic degeneration (in five of five livers) and mild periportal hepatocellular fatty changes (in three of five livers) were present only in rats given 2000 mg/kg/day PMCol. Minimal renal tubule regeneration was found on day 29 in one of six and five of five kidneys from rats treated with 200 and 2000 mg/kg/day PMCol, respectively, and was not detected in the PMCol-treated rats on day 8.

Plasma drug levels. On day 7, the concentration of PMCol in plasma collected 2 h after dose administration was 425 ± 180 ng/ml in the high-dose group. On day 28, plasma drug levels 2 h postdose increased with dose level - 41.5 ± 8.45 ng/ml in 200 mg/kg/day group, and 111 ± 16.9 ng/ml in the 2000 mg/kg/day group.

Metabolomics Analysis

The prevalence of many metabolites was altered in liver, kidney, plasma, and urine after daily administration of PMCol as summarized in Table 2. Individual known metabolites and

TABLE 1
Summary of Selected Clinical Pathology Parameters

A. Serum chemistry values

Dose (mg/kg)	ALT (U/l)	CAL (mg/dl)	CHO (mg/dl)	GLO (g/dl)	GLU (mg/dl)	TBI (mg/dl)	TRI (mg/dl)
Day 8							
0	36 ± 4.1	11.6 ± 0.14	87 ± 12	1.6 ± 0.08	116 ±16.6	0.12 ± 0.02	29 ± 3.0
2000	53 ± 9.5[a]	12.5 ± 0.37[a]	170 ± 31[a]	1.8 ± 0.15[a]	94 ± 6.6[a]	0.24 ± 0.04[a]	38 ± 21
Day 29							
0	39 ± 5.3	12 ± 0.35	93 ± 13.2	2.1 ± 0.14	141 ± 16.3	0.12 ± 0.03	21 ± 5.0
200	40 ± 3.7	12.2± 0.33	126 ± 12.1	1.9 ± 0.20	142 ± 15.8	0.11 ± 0.02	30 ± 6.7
2000	75 ± 16.9[a]	12.8 ± 0.42[a]	218 ± 27[a]	2.1 ± 0.13	125 ± 31.4[a]	0.24 ± 0.03[a]	57 ± 22[a]

B. Hematology values

Dose (mg/kg)	RBC (10^6/μl)	HGB (g/dl)	WBC (10^3/μl)	HCT (%)	AMO (10^3/μl)	PMO (%)	ANS (10^3/μl)	PNS (%)	PLC (10^3/μl)	RET (% RBC)
Day 8										
0	6.8 ± 0.21	13.4 ± 0.45	9.25 ± 2.41	41.1 ± 1.56	0.17 ± 0.05	1.8 ± 0.24	1.05 ± 0.31	11.3 ± 0.97	1258 ± 208	5.35 ± 0.69
2000	6.8 ± 0.25	13.0 ± 0.23	12.15 ± 2.95	39.2 ± 1.13[a]	0.40 ± 0.16[a]	3.2 ± 0.59[a]	1.10 ± 0.34	9.1 ± 2.18[a]	1858 ± 256[a]	4.34 ± 0.96
Day 29										
0	7.88 ± 0.34	14.4 ± 0.46	11.11± 2.01	42.5 ± 1.63	0.23 ± 0.06	2.0 ± 0.30	1.29 ± 0.33	11.5 ± 1.58	852 ± 139	2.47 ± 0.36
200	7.75 ± 0.24	14.1 ± 0.52	9.87 ± 1.64	41.5 ± 1.59	0.20± 0.06	2.0 ± 0.37	1.19 ± 0.32	12.1 ± 3.14	962 ± 123	2.83 ± 0.27
2000	7.14 ± 0.27[a]	13.3 ± 0.49[a]	16.56 ± 1.44[a]	39.5 ± 1.78[a]	0.43 ± 0.08[a]	2.6 ± 0.34[a]	2.17 ± 0.41[a]	13.2 ± 2.87	923 ± 111	3.84 ± 0.36[a]

Note. ALT, Alanine aminotransferase; CAL, calcium; CHO, cholesterol; GLO. globulin; GLU, glucose; TBI, total bilirubin; TRI, and triglycerides. Other parameters included aspartate aminotransferase, alkaline phosphatase, blood urea nitrogen, creatinine, phosphorus, sodium, potassium, chloride, total protein, albumin, and albumin/globulin ratio. RBC, Red blood cell count; HGB, hemoglobin; WBC, total white blood cell count; HCT, hematocrit; AMO, total monocyte; PMO, percent monocyte; ANS, total neutrophil; PNS, percentage neutrophil; PLC, platelet count; RET, percent reticulocyte count. Other parameters included total and percent lymphocyte, eosinophil, and basophil; mean corpuscular hemoglobin, corpuscular volume, corpuscular hemoglobin concentration, and platelet volume; absolute reticulocyte count; and RBC morphology.

[a]Signifies statistically significant differences from the control group.

the fold change with statistical significance identified from liver, kidney, urine, and plasma are presented in Supplementary tables 2–5.

Liver metabolomics. Daily administration with PMCol at 2000 mg/kg/day for both 7 and 28 days depleted hepatic total glutathione in part by inhibiting glutathione biosynthesis (Figs. 2 and 9); however, treatment of rats with 200 mg/kg/day PMCol had essentially no effect on reduced glutathione (GSH) or oxidized glutathione (GSSG) levels. Ophthalmate, a redox-inactive glutathione isostere was also depleted from the tissue of rats treated with 2000 mg/kg/day PMCol. This depletion occurred with concomitant upregulation of the glutamate-cysteine ligase gene (see gene expression analysis below) and accumulation of the component amino acids, especially cysteine (Cys), glycine (Gly) and 2-aminobutyrate. Furthermore, hepatic taurine (downstream product of cysteine) was reduced in PMCol-treated animals compared with the vehicle-treated controls (Supplementary table 2).

PMCol-induced depletion of hepatic glutathione also resulted in redistribution of peripherally associated metabolites including 5-oxoproline and pentose phosphate pathway metabolites such as sedoheptulose-7-phosphate and NAD(P)+ (Figs. 3 and 9). Rats treated with 2000 mg/kg/day for 7 or 28 days showed significant increases in 5-oxoproline, sedoheptulose, and NAD(P)+, whereas levels of cysteine-glutathione disulfide, oxidized glutathione (GSSG) and S-methlyglutathione were decreased. Interestingly, transcripts for glutathione reductase (Gsr), glutathione peroxidase 2 (Gpx2), several glutathione S-transferases, and NAD(P)H dehydrogenase quinone 1 (Nqo1) were all upregulated in response to PMCol (see gene expression analysis below).

Depletion of glutathione by PMCol also affected the hepatic methionine/cysteine distribution (Figs. 4 and 9). Methionine (Met) utilization *via* adenosine conjugation was increased to increase tissue cysteine concentration. Interestingly, the molar equivalent of α-ketobutyrate (α−KB) that was produced upon dissimilation of cystathionine appeared to be funneled into 2−aminobutyrate (2-AB) such that both 2-hydroxybutyrate (AHB) and propionylcarnitine (a surrogate of propionyl-coA) had reduced abundance. The abundance of several cofactors that facilitates these transformations, specifically pyridoxal phosphate (PLP), NAD(P)H, and 5-methyltetrahydrofolate, were altered in conjunction with the observed change in distribution of pathway metabolites.

TABLE 2
Number of Known Metabolites Affected by PMCol Administration

		Number of metabolites at levels statistically different than controls					
		200 mg/kg/day versus vehicle		2000 mg/kg/day versus vehicle			
Tissue	Total number of identified metabolites	day 29		day 8		day 29	
Liver	256	26↑	39↓	45↑	63↓	37↑	75↓
Kidney	270	8↑	15↓	21↑	17↓	28↑	32↓
Urine	240	14↑	51↓	13↑	20↓	31↑	109↓
Plasma	228	26↑	13↓	37↑	38↓	58↑	32↓

Note. Welch's two-sample *t*-test comparisons, $p \leq 0.05$.

The major lipophilic and hydrophilic dietary antioxidants showed reduced hepatic abundance during 7 or 28 days of treatment with 2000 mg/kg/day PMCol. Specifically, α-tocopherol, ascorbate (vitamin C), and ergothionine were significantly reduced as demonstrated in Figure 5.

As shown in Figure 6, daily administration of PMCol at 200 and 2000 mg/kg/day altered normal functions within the liver, specifically lipid biosynthesis and remodeling. In the lipid metabolism pathway, acetylcarnitine was slightly increased on day 8 in the 200 mg/kg/day group and significantly increased in a dose-dependent manner on day 29; malonyl-coA, the downstream product of the acetylcarnitine, was decreased in a dose-dependent manner and was essentially depleted from the liver following 2000 mg/kg/day PMCol treatment. The tissue abundance of squalene also dropped by approximately 50% in rats treated with 2000 mg/kg/day PMCol on both days 8 and 29. There was also a modest but dose-dependent reduction in hepatic cholesterol content in PMCol-treated rats (Fig. 6).

Hepatic xanthine oxidase (XO) activity appeared to have been reduced as evidenced by a dose-dependent reduction in the abundance of each downstream metabolite in the pathway specifically xanthine, urate, and allantoin on day 29 with no change in the abundance of hypoxanthine (the initial substrate). Xanthine, urate, and allantoin were also decreased on day 8 in the 2000 mg/kg/day treatment group (Fig. 7).

Kidney metabolomics. In line with findings in the liver, renal cysteine (and cystine) increased (Supplementary table 3). However, there was no appreciable effect on either methionine or S-adenosylhomocysteine abundance, suggesting that the trans-sulfuration pathway was not induced in the kidney of PMCol-treated rats. Other changes in renal metabolism were not easily linked to observations in the liver and may reflect secondary or tertiary effects downstream of hepatic necrosis. Under the condition of this study, PMCol treatment did not have significant adverse effects on the kidneys.

Urine metabolomics. As stated above, hepatic taurine was reduced in PMCol-treated animals compared with the control group; however, taurine (along with β-alanine) is known to be rapidly exported from hepatocytes into the circulation, and readily filtered by kidneys into the urine. In PMCol-treated animals, both β-alanine and taurine were present in increased abundance in the urine (Supplementary table 4).

Other urine metabolites that are consistent with changes observed in the liver include decreased 3-hydroxy-3-methylglutarate and ascorbate (vitamin C) as well as increased glucuronate and S-adenosylmethione (SAM) (Supplementary table 4).

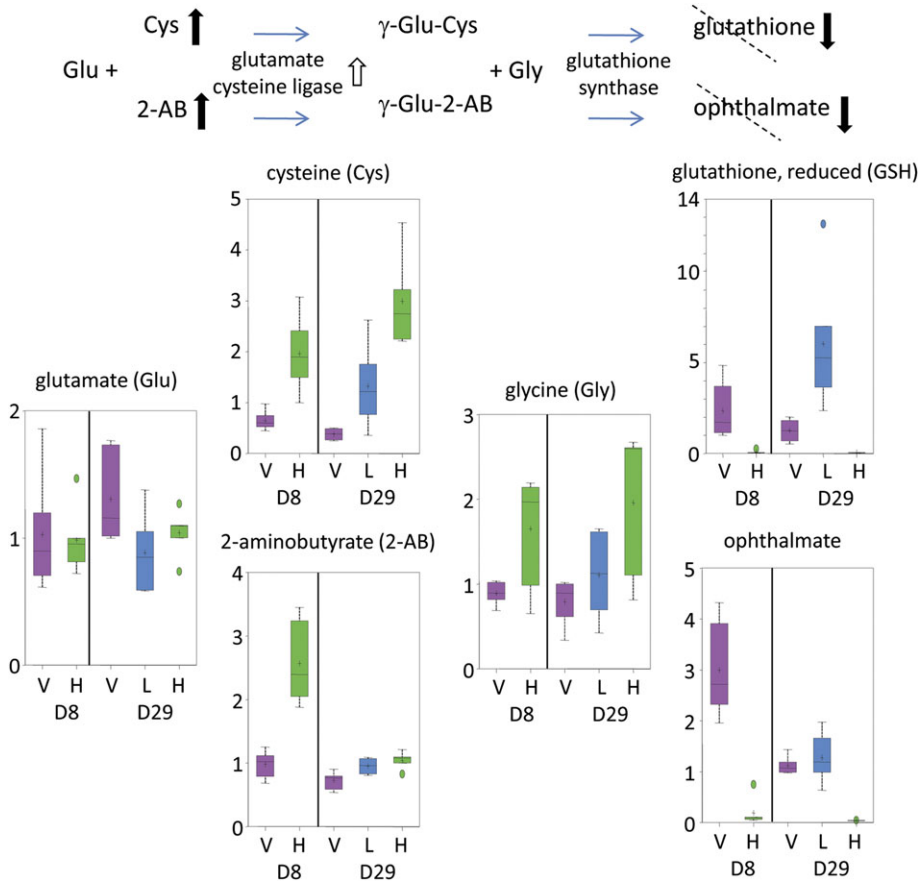

FIG. 2. A condensed illustration of glutathione and ophthalmate biosynthesis with supporting metabolomics data. The metabolomics data for day 8 (D8) and day 29 (D29) rat liver samples are presented as interquartile range box plots. The top and bottom of each box represents the 75th and 25th percentile, respectively. Also shown are the median (—) separating the inner quartiles, the mean (+), ''whiskers'' from the maximum to the minimum, and ''outliers'' (•), which are 1.5× the 1st or 3rd quartile of the data. The y-axis indicates the normalized relative level of the indicated metabolite. V = vehicle control group, H = high-dose group (2000 mg/kg/day), L= low-dose group (200 mg/kg/day). Bold up and down arrows in the biosynthesis pathway indicate increases or decreases, respectively, in the metabolite, whereas hollow arrows indicate differential expression of the enzyme transcript. Metabolites that are reduced to extremely low levels are indicated by a slashed line.

Plasma metabolomics. In concordance with decreased glutathione in the liver, plasma cysteine-glutathione disulfide was decreased in the plasma of the rats treated with 2000 mg/kg/day PMCol (Supplementary table 5). Furthermore, cholesterol as well as metabolites that are transported by Niemann-Pick C1-like 1 (one of the major cholesterol transporters), particularly campesterol and alpha-tocopherol, accumulated in the plasma of PMCol-treated animals, and this accumulation was found to be dose dependent (Fig. 5).

PMCol metabolites. Liver, kidney, plasma, and urine samples, collected for metabolomics, were also examined by LC-MS in the positive- and negative-ion modes for PMCol and possible metabolites. Table 3 summarizes the profile of putative metabolites observed in the high-dose group samples (day 29). The results provided evidence for formation of dehydrogenated and oxidized metabolites, as well as conjugates with sulfate, glucuronide, methyl, and mercapturate. PMCol and seven putative metabolites were detected in the positive ion mode, whereas 25 potential PMCol metabolites were detected using the negative ion mode in tissues, plasma, and urine. Many of these compounds were products of multiple metabolic pathways (e.g., oxidized at one or more sites and then conjugated).

Gene Expression Analysis in Liver

Microarray gene expression analysis was performed on RNA extracted from the livers of each rat (5–6 animals/group). A twofold differential expression change was noted for 18 probe sets (14 upregulated and 4 downregulated) in the 200 mg/kg/day low-dose group on day 29 as compared with the control group. In the 2000 mg/kg/day high-dose group, 211 (107 upregulated and 104 downregulated) and 263 (141 upregulated and 122 downregulated) probes showed a twofold differential expression on day 8 and day 29, respectively, when compared with the control group. Selected genes that were upregulated or downregulated significantly in at least one of the three PMCol-treated

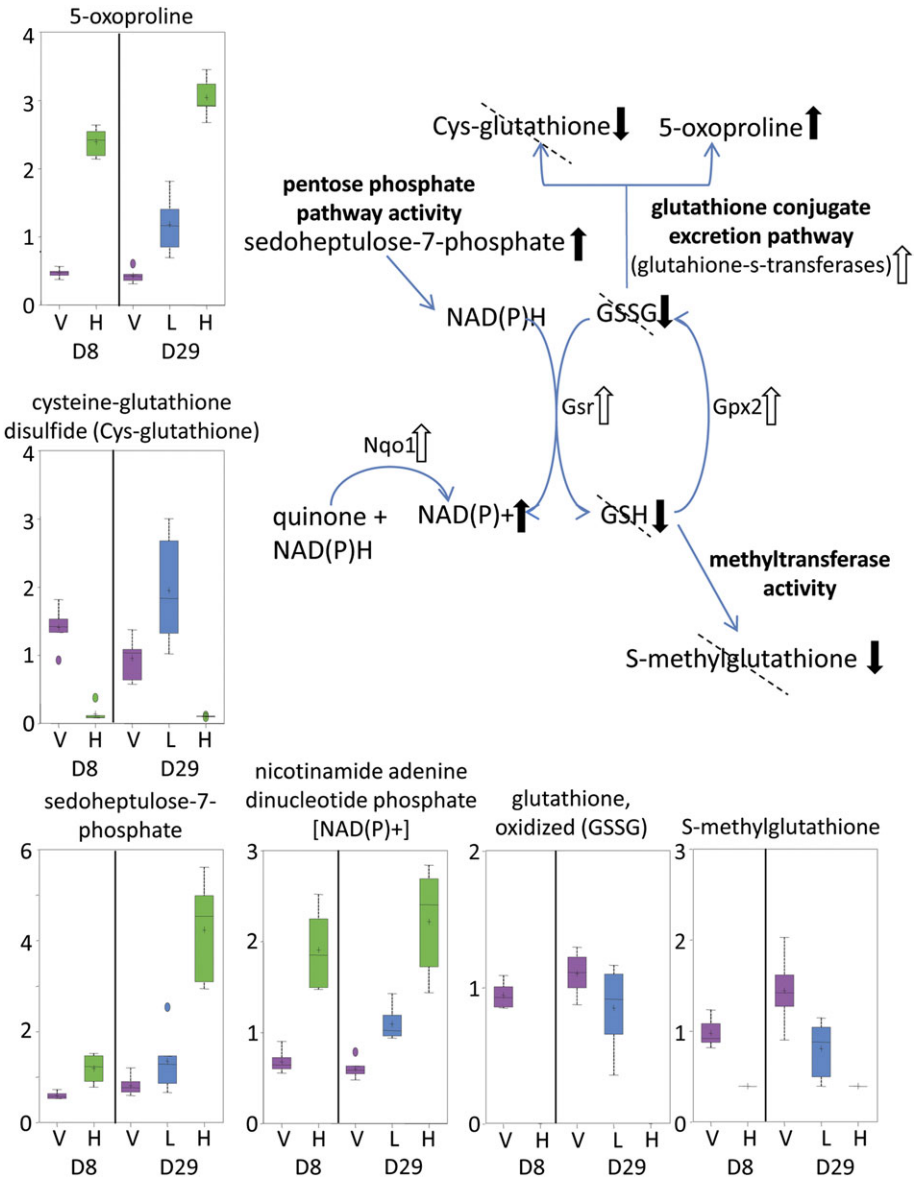

FIG. 3. A condensed illustration of hepatic glutathione depletion and the resulting redistribution of peripherally associated metabolites including 5-oxoproline and pentose phosphate pathway metabolites such as sedoheptulose-7-phosphate after daily PMCol administration. Transcripts for glutathione reductase (Gsr), glutathione peroxidase 2 (Gpx2), several glutathione S-transferases, and NAD(P)H dehydrogenase quinone 1 (Nqo1) were all upregulated in response to PMCol. The explanation for the box plots can be found in the legend of Figure 2.

groups following PMCol administration and their transcriptional fold change for each of the three treatment groups are presented in Table 4. All of the genes had at least twofold differential expression and their upregulated or downregulated fold change values are listed in the Supplemental tables 6–9.

GSEA showed that genes involved in glutathione metabolism and xenobiotic metabolism by cytochrome P450 pathways were the most enriched, and therefore the most perturbed at the transcriptional level following PMCol administration. Multiple glutathione S-transferases, Gpx2, Gsr, and the catalytic and modifier subunits of glutamate-cysteine ligase (Gclc and Gclm, respectively) were all upregulated in the liver after administration of PMCol. In other words, PMCol results in extreme depletion of glutathione and upregulation of genes involved in glutathione synthesis and the glutathione conjugate excretion pathway in the liver of treated rats (see metabolomics results above and Figs. 2 and 3). Furthermore, aldo-keto reductase family 7 member A3 (Akr7a3) and glutathione S-transferase pi1 (Gstp1)—two of the three main biomarkers proposed by Gao and coworkers (Gao *et al.*, 2010) for conjugation-type depletion of glutathione—were upregulated in response to PMCol administration. In addition, OAF homolog *Drosophila* (Oaf), a biomarker of glutathione depletion was similarly downregulated following PMCol administration (Gao *et al.*, 2010).

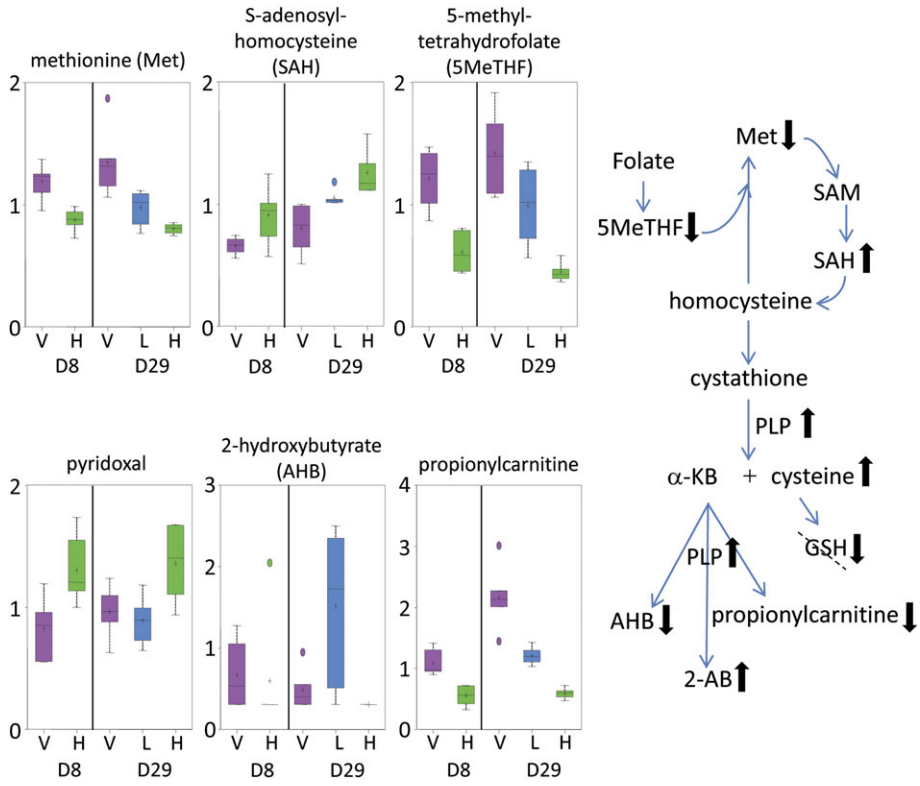

FIG. 4. A condensed illustration of how the methionine-cysteine conversion pathway was affected after daily PMCol administration. The explanation for the box plots can be found in the legend of Figure 2. The box plots for cysteine, 2-aminobutyrate (2-AB), and reduced glutathione (GSH) were previously presented in Figure 2. The molar equivalent of α-ketobutyrate (α-KB) that is produced upon dissimilation of cystathionine appears to be funneled into 2-aminobutyrate (2-AB) with concomitant reductions in 2-hydroxybutyrate (AHB) and propionylcarnitine (a surrogate of propionyl-coA). Despite increases in cysteine, GSH was at extremely low levels. Pyridoxal phosphate (PLP) is involved in transaminations and is synthesized from the nutrient pyridoxal.

Cytochrome P450 (CYP) family members metabolize potentially toxic compounds. Since induction of CYPs has long been known to cause oxidative stress by uncoupling the oxidation of nicotinamide adenine dinucleotide phosphate (NADPH) to generate hydrogen peroxide (Knerr *et al.*, 2006), it is noteworthy that Cyp1a1, Cyp26a1, Cyp2b15, Cyp2b2, and Cyp2c80 genes were upregulated in the liver of rats treated with low and high doses of PMCol. NAD(P)H dehydrogenase quinone 1 (Nqo1), a quinone reductase involved in detoxification pathways, and heme oxygenase 1 (Hmox1), an indicator of cellular oxidative stress (Abraham *et al.*, 2007), were also upregulated in response to PMCol.

Given that PMCol has shown antiandrogenic activity in prostate carcinoma cells and is thought to be a potent chemopreventive agent for androgen-dependent cancers such as prostate cancer (Thompson and Wilding, 2003), the expression of androgen receptor gene (Ar) was evaluated in the liver samples after PMCol treatment. Ar was found to be downregulated by 1.3-fold in response to PMCol at both low- and high-dose levels. PMCol had no notable effect on the expression of genes involved in oxidative phosphorylation or electron transport chain.

To identify potential early gene biomarkers of PMCol toxicity, gene expression results from all three treated groups were compared. This identified 17 genes that were differentially expressed by at least twofold in all groups: Abcc3, Akr7a3, Aldh1a1/Aldh1a7, Aox4, Ces2, Ces5, Ces6, Cryl1, Cyp1a1, Cyp2b15, Cyp2b2, Dusp6, Gsta2/Gsta3/Yc2, Gstt3, Nqo1, Nrg4, and Ugt2b1.

Real-time polymerase chain reaction (qRT-PCR) analysis of day 29 liver transcripts following high and low doses of PMCol for six upregulated genes (Akr7a3, Cyp1a1, Gpx2, Gsr, Gstp1, and Hmox1) and one downregulated gene (Acnat2) confirmed the microarray results (Fig. 8).

DISCUSSION

We applied an integrated approach to study PMCol-induced toxicity by evaluating the compound using classic toxicity endpoints, gene expression, and metabolomics of the liver, kidney, urine, and plasma. PMCol induced periportal hepatocellular hydropic degeneration, cytomegaly, and periportal hepatocellular fatty changes, clearly identifying the liver as the key target for PMCol toxicity.

Glutathione is the predominant intracellular reducing agent in liver. This tripeptide plays a significant role in phase II xenobiotic

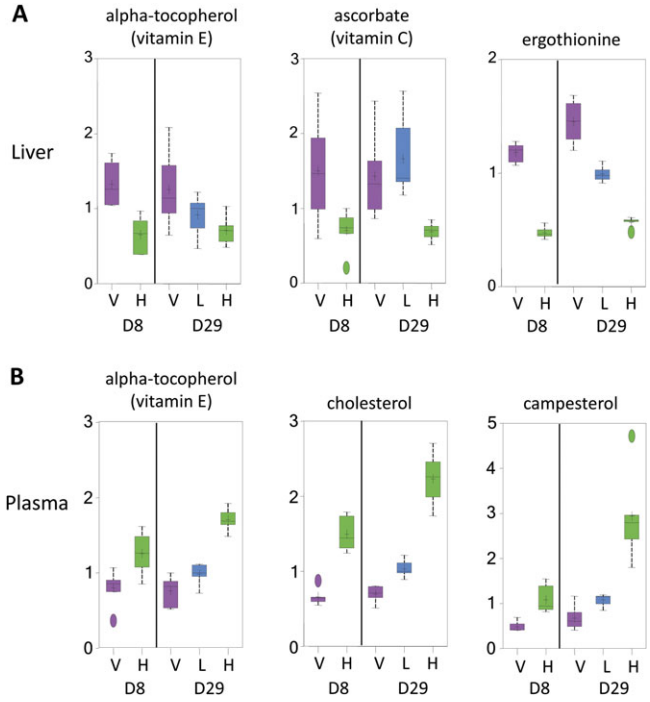

FIG. 5. Daily administration with PMCol reduced the hepatic abundance of dietary antioxidants (panel A) and increased dietary substances in the plasma (panel B). The explanation for the box plots can be found in the legend of Figure 2.

modification and prevents reactive oxygen species (ROS)–mediated oxidative deactivation of cellular proteins. Along with antioxidant enzymes (catalase and superoxide dismutase),

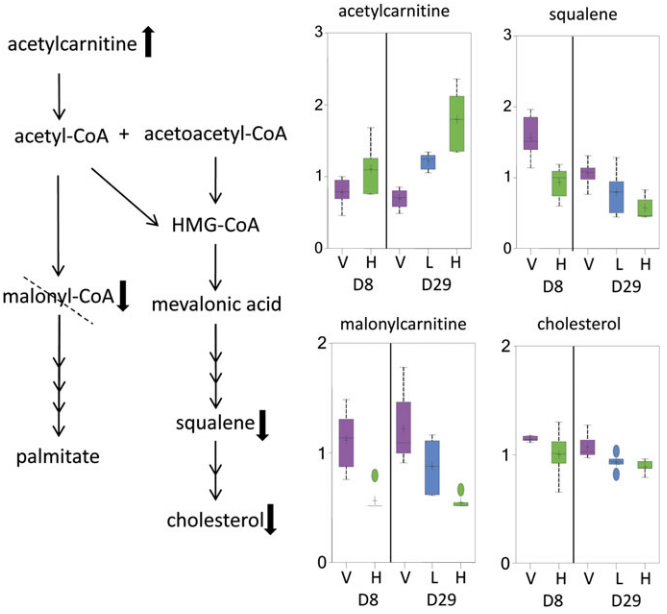

FIG. 6. Daily administration with PMCol altered normal functions within the liver, specifically lipid biosynthesis and remodeling. The explanation for the box plots can be found in the legend of Figure 2. HMG-CoA = 3-hydroxy-3-methylglutaryl-CoA.

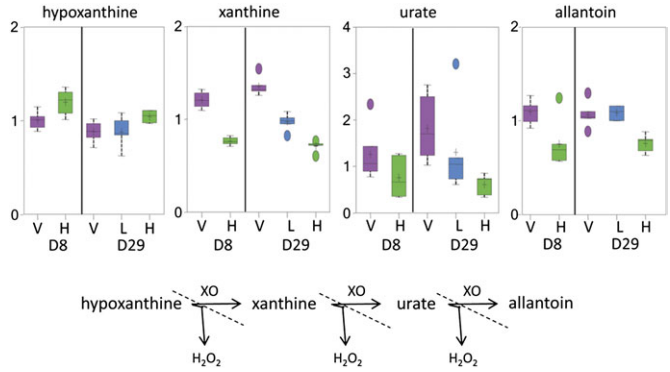

FIG. 7. Daily PMCol treatment reduced the activity of hepatic XO as evidenced by reduced levels of xanthine, urate, and allantoin in the liver. The explanation for the box plots can be found in the legend of Figure 2 with the exception that the slashed line indicates, in this case, inhibition of the XO enzyme.

glutathione maintains cellular redox homeostasis (Pastore *et al.*, 2003). Metabolomic evaluation of liver from PMCol-treated rats demonstrated depletion of both GSH and GSSG in the high-dose group and a concomitant decrease in plasma cys-glutathione disulfide, a marker of hepatic glutathione depletion. Depletion of glutathione also stimulates cysteine biosynthesis (Fig. 9) through the trans-sulfuration pathway, specifically inducing the expression of cystathionine-γ-lyase (Kandil *et al.*, 2010). Dose-dependent decreases in methionine were found after 28 days of PMCol administration, corresponding with increases in both S-adenosylhomocysteine and cysteine (Figs. 4 and 10). Furthermore, ophthalmate, a product of the glutathione synthetic pathway that is not redox reactive, was depleted in the high-dose group. This depletion in glutathione was associated with upregulation of the glutamate-cysteine ligase message and accumulation of the component amino acids, especially cysteine, glycine, and 2-aminobutyrate (Fig. 2)—suggesting inhibition of glutathione biosynthesis by PMCol or its metabolites in a manner analogous to buthionine sulfoximine, a known mechanism-based inhibitor of glutamate-cysteine ligase (gamma glutamylcysteine synthetase) (Griffith and Meister, 1979).

In addition to depletion of liver glutathione, PMCol appeared to compromise hepatic function as evidenced by alterations in sulfur and polyamine metabolism. Metabolomics showed decreases in liver organic sulfates and increases in urinary β-alanine, taurine, and creatine in the high-dose groups; however, the above changes may indirectly be related to increased cysteine production resulting from decreased hepatic glutathione.

PMCol caused oxidative stress as evidenced by appreciable decreases in the cofactor FAD in hepatic tissue after 28 days of treatment, with an increase in the cofactor NAD(P)+ after 7 days (Fig. 3). The increase in NAD(P)+ was associated with an increase in the message for Nqo1, an enzyme that converts NAD(P)H to NAD(P)+ in the presence of reactive quinones (Nebert *et al.*, 2002; Ross *et al.*, 2000). Nqo1 is responsible for conversion of tocopherol quinone, generated from vitamin

TABLE 3
PMCol Putative Metabolites

Putative metabolite[a]	Mass	Mass change	Matrix[b]			
			Liver	Plasma	Kidney	Urine
Positive ion mode						
PMCol (parent drug)	220	0	√	√	√	√
Dehydrogenated (2)	219	−2	√	√	√	√
Dehydrogenated/oxidized/methylated	249	28	√	√		√
2 × hydrogenated/oxidized/methylated	255	34		√		
3 × oxidized/3 × methylated	311	90		√		
Dehydrogenated/glucuronidated	395	174	√	√	√	√
Oxidized/mercapturate	409	188	√	√	√	√
Negative ion mode						
Dehydrogenated/+CO	245	26	√	√	√	√
Dehydrogenated/oxidized/methylated	247	28		√		
Oxidized/methylated	249	30	√	√	√	√
2 × oxidized/methylated (4)	265	46	√	√	√	√
3 × oxidized/methylated	281	62		√	√	√
3 × oxidized/2 × methylated	295	76	√	√	√	√
Sulfated	299	80	√	√	√	√
3 × oxidized/3 × methylated/ hydrogenated	311	92		√	√	√
Dehydrogenated/oxidized/sulfated	313	94	√	√	√	
Oxidized/sulfated (3)	315	96	√	√	√	√
Hydrogenated/oxidized/sulfated	317	98	√	√	√	√
Dehydrogenated/2 × oxidized/sulfated	329	110	√	√	√	√
2 × oxidized/sulfated	331	112	√	√	√	√
Hydrogenated/2 × oxidized/sulfated	333	114	√	√	√	√
Dehydrogenated/3 × oxidized/sulfated	345	126		√		√
Glucuronidated	395	176	√	√	√	√
Hydrogenated/glucuronidated	397	178	√	√		√
Oxidized/glucuronidated (2)	411	192	√	√	√	√
Hydrogenated/oxidized/glucuronidated (2)	413	194	√	√	√	√

[a]Proposed modification to structure listed below. Value in () indicates the number of isobaric metabolites observed.
[b]Tissue or fluid in which putative metabolite was observed.

E chromanol ring interaction with lipid radicals to its hydroquinone (Siegel *et al.*, 1997). Given that PMCol possesses the same chromanol moiety as vitamin E, it may also be converted by lipid peroxy radicals to a reactive quinone and lead to generation of more ROS. Unlike vitamin E, PMCol is more water soluble, less membrane bound, and has more access to the cytosolic glutathione pool. An *in vitro* distribution study demonstrated that after incubation with erythrocytes, PMCol, unlike α-tocopherol, was undetectable in membrane fractions (Koga *et al.*, 1998). Thus, owing to its higher water solubility, PMCol may interact with and deplete cytosolic liver glutathione by both conjugative and non-conjugative mechanisms.

Nqo1 has also been reported to be upregulated in the livers of rats exposed to acetaminophen, carbon tetrachloride, and bromobenzene all of which cause hepatic oxidative stress (Aleksunes *et al.*, 2005; Heijne *et al.*, 2004). Upregulation of Nqo1 during hepatic oxidative stress and damage is an adaptive and protective response to limit progression of liver damage by detoxifying ROS (Aleksunes *et al.*, 2006). Although Nqo1 can convert vitamin E quinone to a hydroquinone, which is known to scavenge superoxide and protect cells from oxidative damage, in our study upregulation of Nqo1 did not appear to protect against liver injury. This may be due in part to a decreased pool of vitamin E in treated rat livers. Our metabolomic data showed that the liver vitamin E pool was significantly decreased even though vitamin E was significantly increased in the plasma of rats treated with low and high doses of PMCol. Given the structural similarity between PMCol and vitamin E, it is possible that PMCol results in depletion of liver vitamin E by inhibiting its liver absorption and/or interfering with its cell membrane incorporation, thereby, preventing the protective effect of Nqo1 and leading to cell damage.

Based on the metabolomic data, PMCol competes with vitamin E and campesterol (a dietary metabolite) for cellular uptake. Vitamin E, campesterol, and cholesterol are transported by one of the major cholesterol transporters, Niemann-Pick C1-

TABLE 4
Transcriptional Fold Changes in Liver after PMCol Administration

Probeset Id.	Gene symbol	Gene name	Fold change		
			Low dose, day 29	High dose, day 29	High dose, day 8
Upregulated genes					
10746293	Abcc3	ATP-binding cassette, subfamily C (CFTR/MRP), member 3	8.63	21.13	11.66
10714323	Aldh1a1|Aldh1a7	Aldehyde dehydrogenase one family,	2.18	3.32	2.69
10729284		member A1|aldehyde dehydrogenase family 1, subfamily A7	4.27	27.93	15.65
10854417	Akr1b10	Aldo-keto reductase family 1, member B10 (aldose reductase)	1.00	2.28	1.80
10854427	Akr1b7	Aldo-keto reductase family 1, member B7	1.15	13.75	6.45
10854406	Akr1b8	Aldo-keto reductase family 1, member B8	1.10	31.37	19.18
10873387	Akr7a3	Aldo-keto reductase family 7, member A3 (aflatoxin aldehyde reductase)	2.78	6.32	6.50
10860951	Asns	Asparagine synthetase	1.95	6.46	5.95
10716509	Ces2	Carboxylesterase 2 (intestine, liver)	5.41	13.13	9.11
10805614	Ces5	Carboxylesterase 5	3.33	6.15	2.66
10808984	Ces6	Carboxylesterase 6	2.23	4.55	3.04
10716502	RGD1565045_predicted	Similar to carboxylesterase isoenzyme gene (predicted)	1.58	3.43	2.64
10784125	Cryl1	Crystalline, lambda 1	2.81	3.51	3.73
10789301	Csmd1	CUB and Sushi multiple domains 1	1.84	4.88	5.11
10910376	Cyp1a1	Cytochrome P450, family 1, subfamily a, polypeptide 1	2.79	4.78	2.64
10729890	Cyp26a1	Cytochrome P450, family 26, subfamily A, polypeptide 1	1.48	2.86	1.79
10705225	Cyp2b15|LOC687222	Cytochrome P450, family 2, subfamily b, polypeptide 15|similar to Cytochrome P450 2B12 (CYPIIB12)	3.43	3.96	3.21
10705230	Cyp2b2	Cytochrome P450, family 2, subfamily b, polypeptide 2	3.58	4.73	3.76
10730031	Cyp2c80_predicted	Cytochrome P450, family 2, subfamily c, polypeptide 80	1.58	8.85	6.16
10880415	Dhdds	Dehydrodolichyl diphosphate synthase	1.52	1.55	1.46
10770342	Ephx1	Epoxide hydrolase 1, microsomal	1.42	1.78	1.86
10911747	Gclc	Glutamate-cysteine ligase, catalytic subunit	1.26	1.91	1.75
10818793	Gclm	Glutamate-cysteine ligase, modifier subunit	1.10	1.65	1.80
10714214	Gna14	Guanine nucleotide binding protein, alpha 14	1.49	2.47	1.26
10853229	Gnai1	Guanine nucleotide binding protein (G protein), alpha inhibiting 1	1.90	3.24	3.14
10890729	Gpx2	Glutathione peroxidase 2	1.17	1.81	2.59
10748891	Grin2c	Glutamate receptor, ionotropic, *N*-methyl D-aspartate 2C	1.10	3.98	2.72
10911802	Gsta2|Gsta3|LOC494499|Yc2	Glutathione S-transferase, alpha	1.55	2.72	3.03
10922151		type2|glutathione S-transferase A3|LOC494499 protein|glutathione S-transferase Yc2 subunit	5.91	15.96	10.61
10911797	Gsta4	Glutathione S-transferase, alpha 4	1.07	2.05	1.94
10792061	Gsr	Glutathione reductase	1.38	2.21	2.09
10727429	Gstp1	Glutathione S-transferase, pi 1	1.30	5.12	4.72
10832555	Gstt1	Glutathione S-transferase theta 1	1.47	2.00	1.90
10832563	Gstt3	glutathione S-transferase, theta 3	2.00	3.34	3.22
10806122	Hmox1	Heme oxygenase (decycling) 1	1.43	2.45	2.21
10790966	Isyna1	Inositol-3-phosphate synthase 1	1.31	2.47	2.43
10919103	Me1	Malic enzyme 1, NADP(+)-dependent, cytosolic	1.68	4.16	3.58
10815308	Mgst2_predicted	Microsomal glutathione S-transferase 2	1.44	2.13	2.06

TABLE 4—*Continued*

Probeset Id.	Gene symbol	Gene name	Fold change		
			Low dose, day 29	High dose, day 29	High dose, day 8
10810867	Nqo1	NAD(P)H dehydrogenase, quinone 1	2.22	6.11	4.73
10788627	Nrg1	Neuregulin 1	1.77	2.49	2.55
10917617	Nrg4	Neuregulin 4	2.22	2.61	2.32
10937734	Pir	Pirin (iron-binding nuclear protein)	1.61	2.58	2.65
10729096	Psat1	Phosphoserine aminotransferase 1	1.21	2.49	3.70
10749716	Pycr1_predicted	Pyrroline-5-carboxylate reductase 1	1.27	2.19	1.63
10739558	Slc16a5| Armc7	Solute carrier family 16, member 5 (monocarboxylic acid transporter 6)''///'' armadillo repeat containing 7	1.46	8.84	8.58
10739323	Slc16a6	Solute carrier family 16, member 6 (monocarboxylic acid transporter 7)	1.48	2.39	2.07
10795218	Slc17a3	Solute carrier family 17 (sodium phosphate), member 3	1.65	3.57	2.94
10902578	Slc35e3	Solute carrier family 35, member E3	1.22	2.09	1.89
10811531.	Slc7a5.	Solute carrier family 7 (cationic amino acid transporter, y+ system), member 5	1.00	2.58	2.65
10771988	Ugt2b17	UDP glucuronosyltransferase 2 family, polypeptide B17	2.36	3.17	3.61
10871588	Zmynd12_predicted	Zinc finger, MYND domain containing 12 (predicted)	1.32	2.04	2.27
Downregulated genes					
10876703	Acnat2|LOC313220	Similar to bile acid Coenzyme A: amino acid	1.45	5.67	8.92
10876707		N-acyltransferase; glycine N-choloyltransferase	1.45	5.58	7.23
10923432	Aox3	Aldehyde oxidase 3	1.97	3.30	6.94
10923474	Aox4	Aldehyde oxidase 4	3.20	3.21	2.12
10923476			1.74	2.51	3.97
10895747	Avpr1a	Arginine vasopressin receptor 1A.	1.53	1.49	2.35
10895144	Dusp6	Dual specificity phosphatase 6.	2.42	3.38	3.00
10825362	Hao2	Hydroxyacid oxidase 2 (long chain)	1.33	3.38	3.70
10928813	Mreg	Melanoregulin	1.19	1.89	2.01
10902249	Nav3	Neuron navigator 3	1.40	2.03	1.54
10902280			1.67	2.64	2.11
10902282			1.54	2.51	2.06
10708485	Nox4	NADPH oxidase 4	1.43	5.37	6.58
10916659	Oaf	OAF homolog (Drosophila)	1.59	2.20	2.36
10726280	Oat	Ornithine aminotransferase	1.61	3.07	3.53
10936637	Rgn	Regucalcin	1.56	1.88	2.75

Note. Genes of interest with at least 1.5-fold differential expression (compared with controls) in at least one of the three experimental treatment groups. Each of the listed genes had gene expression levels in the high-dose group on days 8 and 29 that were altered with statistical significance (*T*-test with Benjamini-Hochberg Multiple Testing Correction, corrected p value ≤ 0.05) when compared with their respective control group.

like 1(Abuasal *et al*., 2010; Narushima *et al*., 2008; Takada and Suzuki, 2010). Furthermore, major lipophilic and hydrophilic dietary antioxidants and ergothionine (a highly abundant fungal metabolite in erythrocytes) showed reduced hepatic abundance with high doses of PMCol (Fig. 5). The role of ergothionine as an antiapoptotic agent and the identification of its transporter, ETT, have only recently been elucidated (Paul and Snyder, 2010). Oxidized ergothionine is a strong reducing agent and until intracellular glutathione is depleted, reduced ergothionine is functionally inert.

During lipid biosynthesis, the liver generates palmitate and cholesterol from excess citrate, producing cytosolic acetyl-coA, acetoacetyl-coA, and malonyl-coA. In this study, PMCol administration altered normal liver function, specifically lipid biosynthesis and remodeling. Inhibition of lipid anabolism by PMCol is evidenced by depletion of malonyl-CoA and decreases in squalene and hepatic cholesterol (Fig. 6). Furthermore, PMCol caused an increase in the level of hepatic acetylcarnitine, indicating inhibition of acetyl-coA incorporation into these pathways.

Hepatic XO, which carries out successive oxidation of hypoxanthine to allantoin and generates hydrogen peroxide at each step, may also play a role in the PMCol-induced hepatotoxicity. The lower abundance of each downstream

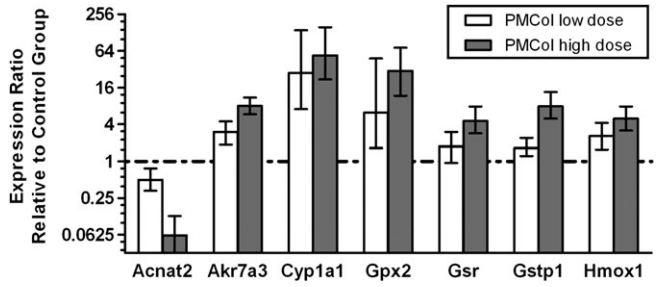

FIG. 8. qRT-PCR expression ratios for seven genes expressed in the liver after 28 daily doses (200 mg/kg low dose or 2000 mg/kg high dose) of PMCol. Data are represented as upregulated or downregulated in comparison with the vehicle control group by a mean factor ± SEM, $n = 5$ group and normalized to Gapdh expression levels for each sample. Upregulated genes have expression ratios > 1.0 and the downregulated gene Acnat2 has expression ratios < 1.0. The expression level for each of the seven genes is statistically different from that of the control group using the hypothesis test in the REST 2009 Software ($p \leq 0.01$).

metabolite (specifically xanthine, urate, and allantoin) in the XO pathway with no change in the initial substrate (hypoxanthine) suggests that PMCol decreases hepatic XO activity (Fig. 7).

Toxicogenomic results were consistent with metabolomic findings, indicating that PMCol-hepatotoxicity is related to glutathione depletion. Various genes in the glutathione metabolic pathway were significantly affected (upregulated or downregulated) by PMCol. Two previously described biomarkers of hepatotoxicity induced by a conjugation-based mechanism of glutathione depletion—aldo-keto reductase family 7 member A3 (Akr7a3) and glutathione S-transferase, pi 1 (Gstp1) (Gao *et al.*, 2010)—were upregulated in liver after PMCol administration.

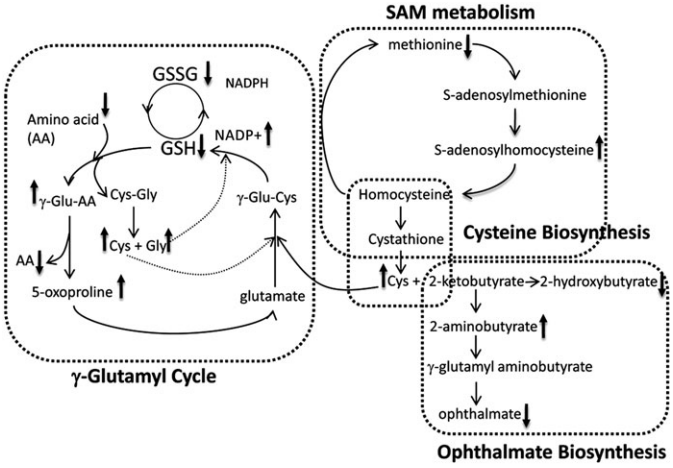

FIG. 9. Illustration of biochemical pathways affected by PMCol administration. Abbreviations are as follows. SAM =S-adenosylmethione, Cys = cysteine, GSH = reduced glutathione, GSSG = oxidized glutathione, Gly = glycine, Cys-Gly = cysteinylglycine, γ -Glu-AA = γ-5-L-glutamyl-L-amino acid, and γ -Glu-Cys = γ-glutamylcysteine.

The genomics data also indicated altered expression of the CYP genes; several CYPs were upregulated, whereas others were downregulated. Additionally, PMCol plasma levels were reduced on day 28 compared with day 7 suggesting that PMCol may induce CYPs responsible for its own metabolism, leading to generation of glutathione conjugated intermediates of PMCol metabolite(s). The *in vitro* and *in vivo* metabolism of PMCol has been reported (Gorman *et al.*, 2009), and the main metabolites formed by rats were the dehydrogenated-sulfate, oxidized glucuronide, dehyrogenated glucuronide, sulfate, and glucuronide conjugates. In the current study, these metabolites were observed, as well as several others. More than 30 different putative PMCol metabolites were detected by LC-MS in tissues, plasma, and urine from PMCol-treated rats (Table 3). PMCol was primarily oxidized or dehydrogenated (probable products of CYPs) and further metabolized to sulfate, glucuronide, or methylated conjugates. One metabolite found in liver and plasma is a mercapturate of an oxidized form of PMCol, suggesting that glutathione conjugation of a PMCol metabolite may be partially responsible for glutathione depletion.

Induction of CYPs causes oxidative stress by uncoupling oxidation of NADPH to generate hydrogen peroxide (Bondy and Naderi, 1994). ROS may be formed by auto-oxidation of the oxycytochrome P450 complex, generating superoxide, which in turn is converted to hydrogen peroxide by superoxide dismutase and catalase. Induction of CYP1A1 by chemicals has also been shown to cause ROS formation and lead to oxidative stress (Knerr *et al.*, 2006), likely by metabolizing the membrane lipid arachidonic acid to stable biologically active epoxides (Diani-Moore *et al.*, 2006; Rifkind, 2006), thereby causing excessive lipid peroxidation and ROS formation. In this study, PMCol upregulated CYP1A1 gene and the oxidative stress biomarker gene, Hmox1. Although Jackson *et al.* (2009) suggested that PMCol does not induce CYPs *in vitro* and drug-drug interaction with PMCol is minimal, the panel of CYPs used in their study only included CYP 1A2, 2B6, and 3A4. Toxicogenomic data from the current study supports their findings but also indicates that PMCol can upregulate transcription of various other CYPs.

Based on the metabolomic and toxicogenomic evaluations, changes in several metabolic products (particularly, methionine, cysteine, and glutathione) and genes (specifically, Akr7a3, Gstp1, and CYPs) in the glutathione metabolism pathway may be potential early markers of PMCol-induced hepatotoxicity. Additionally, the 17 genes differentially expressed by at least twofold in all PMCol-treated groups may serve, upon further investigation, as early markers of PMCol-induced hepatotoxicity.

In contrast to earlier published data (Lindeblad *et al.*, 2010a), we report minor renal histopathology findings and no PMCol-attributable clinical chemistry changes indicative of kidney damage. Metabolomics results were inconclusive with respect to PMCol-induced kidney injury, and microscopic examination of the kidney showed slight renal tubular regeneration in rats given low and high doses of PMCol.

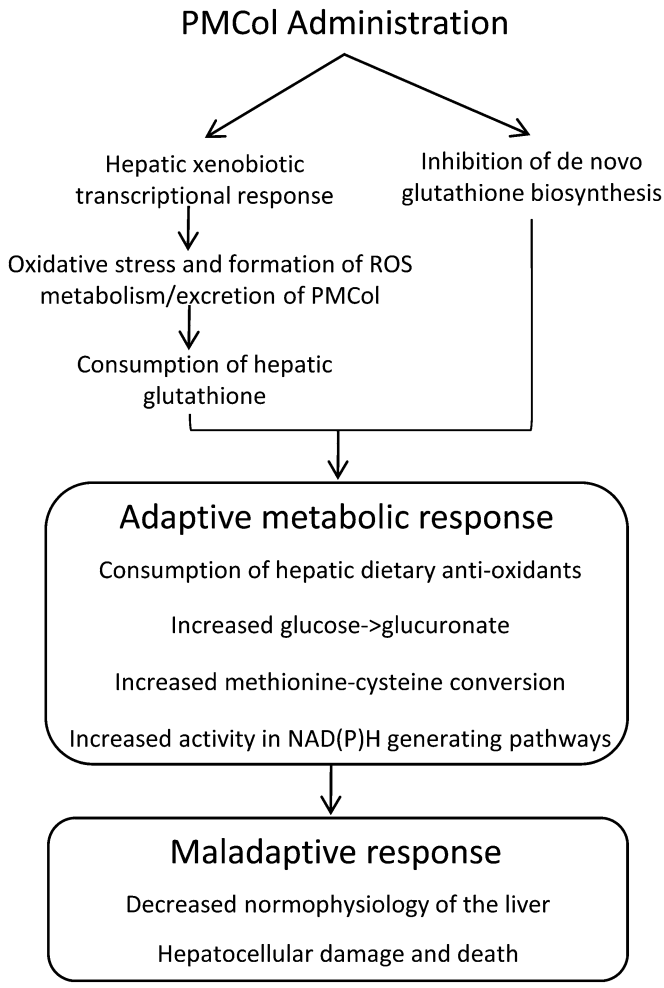

FIG. 10. Cascade of events and responses following daily PMCol administration.

In summary, administration of PMCol depletes total glutathione in part by inhibition of its biosynthesis as evidenced by alterations in cellular metabolites within glutathione biosynthesis pathway (Fig. 9). PMCol also alters hepatic function and hepatic xenobiotic transcriptional response which in turn may lead to bioactivation of PMCol to an intermediate that may generate ROS and further consumption of hepatic glutathione (Fig. 10). Depletion of glutathione ultimately yields an adaptive metabolic response with the consumption of hepatic dietary antioxidants, increased methionine to cysteine conversion, and increases NAD(P)+ production—a maladaptive response demonstrated by decreased normophysiology of the liver, hepatocellular damage and death.

Integration of data generated by standard toxicology endpoints with metabolomics and genomics details the impact of daily administration of high doses of PMCol. PMCol-induced liver damage and dysfunction is likely due to glutathione depletion from inhibition of synthesis, depletion of liver glutathione, and modification of other drug metabolism pathways. Understanding the function of upregulated genes and bioactivation of PMCol by CYPs may elucidate the mechanism of action and provide early markers of toxicity of vitamin E-like chemopreventive agents.

SUPPLEMENTARY DATA

Supplementary data are available online at http://toxsci.oxfordjournals.org/.

FUNDING

This work was supported in whole or in part by federal funds from the Chemopreventive Agent Development Research Group at the National Cancer Institutes of Health, Department of Health and Human Services (HHSN26120043005C).

ACKNOWLEDGMENTS

We thank Elizabeth Zuo and Michael Eckart at the Stanford University Protein and Nucleic Acid Facility for the hybridization and image scan of Affymetrix microarray chips and SRI International's toxicology services personnel, especially Todd Louketis, for their assistance during the in-life portion of the study.

REFERENCES

Abdo, K. M., Rao, G., Montgomery, C. A., Dinowitz, M., and Kanagalingam, K. (1986). Thirteen-week toxicity study of d-alpha-tocopheryl acetate (vitamin E) in Fischer 344 rats. *Food Chem. Toxicol.* **24,** 1043–1050.

Abraham, N. G., Asija, A., Drummond, G., and Peterson, S. (2007). Heme oxygenase -1 gene therapy: Recent advances and therapeutic applications. *Curr. Gene Ther.* **7,** 89–108.

Abuasal, B., Sylvester, P. W., and Kaddoumi, A. (2010). Intestinal absorption of gamma-tocotrienol is mediated by Niemann-Pick C1-like 1: In situ rat intestinal perfusion studies. *Drug Metab. Dispos.* **38,** 939–945.

Aleksunes, L. M., Goedken, M., and Manautou, J. E. (2006). Up-regulation of NAD(P)H quinone oxidoreductase 1 during human liver injury. *World J. Gastroenterol.* **12,** 1937–1940.

Aleksunes, L. M., Slitt, A. M., Cherrington, N. J., Thibodeau, M. S., Klaassen, C. D., and Manautou, J. E. (2005). Differential expression of mouse hepatic transporter genes in response to acetaminophen and carbon tetrachloride. *Toxicol. Sci.* **83,** 44–52.

Bondy, S. C., and Naderi, S. (1994). Contribution of hepatic cytochrome P450 systems to the generation of reactive oxygen species. *Biochem. Pharmacol.* **48,** 155–159.

Boudonck, K. J., Rose, D. J., Karoly, E. D., Lee, D. P., Lawton, K. A., and Lapinskas, P. J. (2009). Metabolomics for early detection of drug-induced kidney injury: Review of the current status. *Bioanalysis* **1,** 1645–1663.

Diani-Moore, S., Papachristou, F., Labitzke, E., and Rifkind, A. B. (2006). Induction of CYP1A and cyp2-mediated arachidonic acid epoxygenation and suppression of 20-hydroxyeicosatetraenoic acid by imidazole derivatives including the aromatase inhibitor vorozole. *Drug Metab. Dispos.* **34,** 1376–1385.

Evans, A. M., DeHaven, C. D., Barrett, T., Mitchell, M., and Milgram, E. (2009). Integrated, nontargeted ultrahigh performance liquid chromatography/electrospray ionization tandem mass spectrometry platform for the identification and relative quantification of the small-molecule complement of biological systems. *Anal. Chem.* **81,** 6656–6667.

Gao, W., Mizukawa, Y., Nakatsu, N., Minowa, Y., Yamada, H., Ohno, Y., and Urushidani, T. (2010). Mechanism-based biomarker gene sets for glutathione depletion-related hepatotoxicity in rats. *Toxicol. Appl. Pharmacol.* **247,** 211–221.

Gorman, G. S., Coward, L., Kerstner-Wood, C., Freeman, L., Hébert, C. D., and Kapetanovic, I. M. (2009). In-vitro and in-vivo metabolic studies of the candidate chemopreventative pentamethylchromanol using liquid chromatography/tandem mass spectrometry. *J. Pharm. Pharmacol.* **61,** 1309–1318.

Gregor, W., Grabner, G., Adelwohrer, C., Rosenau, T., and Gille, L. (2005). Antioxidant properties of natural and synthetic chromanol derivatives: Study by fast kinetics and electron spin resonance spectroscopy. *J. Org. Chem.* **70,** 3472–3483.

Griffith, O. W., and Meister, A. (1979). Potent and specific inhibition of glutathione synthesis by buthionine sulfoximine (S-n-butyl homocysteine sulfoximine). *J. Biol. Chem.* **254,** 7558–7560.

Heijne, W. H., Slitt, A. L., van Bladeren, P. J., Groten, J. P., Klaassen, C. D., Stierum, R. H., and van Ommen, B. (2004). Bromobenzene-induced hepatotoxicity at the transcriptome level. *Toxicol. Sci.* **79,** 411–422.

Jackson, J. P., Kabirov, K. K., Kapetanovic, I. M., and Lyubimov, A. (2009). In vitro assessment of P450 induction potential of novel chemopreventive agents SR13668, 9-cis-UAB30, and pentamethychromanol in primary cultures of human hepatocytes. *Chem. Biol. Interact.* **179,** 263–272.

Kandil, S., Brennan, L., and McBean, G. J. (2010). Glutathione depletion causes a JNK and p38MAPK-mediated increase in expression of cystathionine-gamma-lyase and upregulation of the transsulfuration pathway in C6 glioma cells. *Neurochem. Int.* **56,** 611–619.

Knerr, S., Schaefer, J., Both, S., Mally, A., Dekant, W., and Schrenk, D. (2006). 2,3,7,8-Tetrachlorodibenzo-p-dioxin induced cytochrome P450s alter the formation of reactive oxygen species in liver cells. *Mol. Nutr. Food Res.* **50,** 378–384.

Koga, T., Moro, K., and Terao, J. (1998). Protective effect of a vitamin E analog, phosphatidylchromanol, against oxidative hemolysis of human erythrocytes. *Lipids* **33,** 589–595.

Liang, D., Lin, J., Grossman, H. B., Ma, J., Wei, B., Dinney, C. P., and Wu, X. (2008). Plasma vitamins E and A and risk of bladder cancer: A case-control analysis. *Cancer Causes Control* **19,** 981–992.

Lindeblad, M., Kapetanovic, I. M., Kabirov, K. K., Detrisac, C. J., Dinger, N., Mankovskaya, I., Zakharov, A., and Lyubimov, A. V. (2010a). Assessment of oral toxicity and safety of pentamethylchromanol (PMCol), a potential chemopreventative agent, in rats and dogs. *Toxicology* **273,** 19–28.

Lindeblad, M. O., Bauer, K. S., Zakharov, A. D., Hill, J. M., Green, J. S., Thomas, B. F., Schwartz, A., Kapetanovic, I. M., and Lyubimov, A. (2010b). Pharmacokinetic and tissue distribution study of [14C]fluasterone in male Beagle dogs following intravenous, oral and subcutaneous dosing routes. *Chem. Biol. Interact.* **183,** 317–326.

Narushima, K., Takada, T., Yamanashi, Y., and Suzuki, H. (2008). Niemann-pick C1-like 1 mediates alpha-tocopherol transport. *Mol. Pharmacol.* **74,** 42–49.

Nebert, D. W., Roe, A. L., Vandale, S. E., Bingham, E., and Oakley, G. G. (2002). NAD(P)H:quinone oxidoreductase (NQO1) polymorphism, exposure to benzene, and predisposition to disease: A HuGE review. *Genet. Med.* **4,** 62–70.

Pastore, A., Federici, G., Bertini, E., and Piemonte, F. (2003). Analysis of glutathione: Implication in redox and detoxification. *Clin. Chim. Acta* **333,** 19–39.

Paul, B. D., and Snyder, S. H. (2010). The unusual amino acid L-ergothioneine is a physiologic cytoprotectant. *Cell Death Differ.* **17,** 1134–1140.

Pfaffl, M. W. (2001). A new mathematical model for relative quantification in real-time RT-PCR. *Nucleic Acids Res.* **29,** e45.

Pfaffl, M. W., Horgan, G. W., and Dempfle, L. (2002). Relative expression software tool (REST) for group-wise comparison and statistical analysis of relative expression results in real-time PCR. *Nucleic Acids Res.* **30,** e36.

Rifkind, A. B. (2006). CYP1A in TCDD toxicity and in physiology-with particular reference to CYP dependent arachidonic acid metabolism and other endogenous substrates. *Drug Metab. Rev.* **38,** 291–335.

Ross, D., Kepa, J. K., Winski, S. L., Beall, H. D., Anwar, A., and Siegel, D. (2000). NAD(P)H:quinone oxidoreductase 1 (NQO1): Chemoprotection, bioactivation, gene regulation and genetic polymorphisms. *Chem. Biol. Interact.* **129,** 77–97.

Sha, W., da Costa, K. A., Fischer, L. M., Milburn, M. V., Lawton, K. A., Berger, A., Jia, W., and Zeisel, S. H. (2010). Metabolomic profiling can predict which humans will develop liver dysfunction when deprived of dietary choline. *FASEB J.* **24,** 2962–2975.

Sharhar, S., Normah, H., Fatimah, A., Fadilah, R. N., Rohi, G. A., Amin, I., Cham, B. G., Rizal, R. M., and Fairulnizal, M. N. (2008). Antioxidant intake and status, and oxidative stress in relation to breast cancer risk: A case-control study. *Asian Pac. J. Cancer Prev.* **9,** 343–349.

Shen, J., Gammon, M. D., Terry, M. B., Teitelbaum, S. L., Eng, S. M., Neugut, A. I., and Santella, R. M. (2008). Xeroderma pigmentosum complementation group C genotypes/diplotypes play no independent or interaction role with polycyclic aromatic hydrocarbons-DNA adducts for breast cancer risk. *Eur. J. Cancer* **44,** 710–717.

Siegel, D., Bolton, E. M., Burr, J. A., Liebler, D. C., and Ross, D. (1997). The reduction of alpha-tocopherolquinone by human NAD(P)H: Quinone oxidoreductase: The role of alpha-tocopherolhydroquinone as a cellular antioxidant. *Mol. Pharmacol.* **52,** 300–305.

Suh, N., Paul, S., Lee, H. J., Ji, Y., Lee, M. J., Yang, C. S., Reddy, B. S., and Newmark, H. L. (2007). Mixed tocopherols inhibit N-methyl-N-nitrosourea-induced mammary tumor growth in rats. *Nutr. Cancer* **59,** 76–81.

Takada, T., and Suzuki, H. (2010). Molecular mechanisms of membrane transport of vitamin E. *Mol. Nutr. Food Res.* **54,** 616–622.

Takei, M., Ando, Y., Saitoh, W., Tanimoto, T., Kiyosawa, N., Manabe, S., Sanbuissho, A., Okazaki, O., Iwabuchi, H., Yamoto, T., *et al.* (2010). Ethylene glycol monomethyl ether-induced toxicity is mediated through the inhibition of flavoprotein dehydrogenase enzyme family. *Toxicol. Sci.* **118,** 643–652.

Thompson, T. A., and Wilding, G. (2003). Androgen antagonist activity by the antioxidant moiety of vitamin E, 2,2,5,7,8-pentamethyl-6-chromanol in human prostate carcinoma cells. *Mol. Cancer Ther.* **2,** 797–803.

Tyurina, Y. Y., Tyurin, V. A., Yalowich, J. C., Quinn, P. J., Claycamp, H. G., Schor, N. F., Pitt, B. R., and Kagan, V. E. (1995). Phenoxyl radicals of etoposide (VP-16) can directly oxidize intracellular thiols: Protective versus damaging effects of phenolic antioxidants. *Toxicol. Appl. Pharmacol.* **131,** 277–288.